

Engineering
Electrical Engineering fields

Okayama University

Year 1996

Measurement and reduction of EMI
radiated by a PWM inverter-fed AC
motor drive system

Satoshi Ogasawara
Okayama University

Hideki Ayano
Okayama University

Hirofumi Akagi
Okayama University

This paper is posted at eScholarship@OUDIR : Okayama University Digital Information Repository.

http://escholarship.lib.okayama-u.ac.jp/electrical_engineering/26

Measurement and Reduction of EMI Radiated by a PWM Inverter-Fed AC Motor Drive System

Satoshi Ogasawara, *Member, IEEE*, Hideki Ayano and Hirofumi Akagi *Fellow, IEEE*
Okayama University
3-1-1 Tsushima-Naka, Okayama, 700 JAPAN

Abstract—This paper presents theoretical and experimental relationships in between radiated electromagnetic noises and common-mode and normal-mode currents, paying attention to an induction motor drive system fed by a voltage-source PWM inverter. A method of reducing both the currents is proposed, based on an equivalent model taking parasitic stray capacitors inside an induction motor into account. Electro-Magnetic Interference (EMI) radiated by a 3.7kW induction motor drive system is actually measured, complying with the VDE 0871 Class A [3m]. Experimental results verify that the combination of the already proposed common-mode transformer and the normal-mode filters being proposed in this paper is a practically viable and effective way to reduce the EMI resulting from both the common-mode and normal-mode currents.

I. INTRODUCTION

PROGRESS of high-speed switching devices such as IGBT's has enabled us to increase the carrier frequency of voltage-source PWM inverters, thus leading to much better operating characteristics. High-speed switching, however, can accompany the following serious problems originating from a step voltage/current change:

- ground current escaping to the earth through stray capacitors inside motors[1][2]
- conducted and radiated EMI[3]–[5]
- bearing current and shaft voltage[6][7]
- shortening of insulation life of motors and transformers[8]–[11]

The step voltage/current change caused by high-speed switching produces high-frequency oscillatory common-mode and normal-mode currents at the instant of every switching, because parasitic stray capacitors inevitably exist inside an ac motor. The oscillatory currents with a frequency range of 100kHz to several MHz can create a magnetic field, and radiate Electro-Magnetic Interference (EMI) noises throughout, thus having a bad effect on electronic devices such as AM radio receivers and medical equipment. However, few literatures have been reported on the EMI noises radiated by power electronic equipment.

This paper presents theoretical and experimental relationships between the radiated EMI noises and the high-frequency oscillatory common-mode and normal-mode currents, paying attention to an induction motor drive system fed by a voltage-source PWM inverter. A method of reducing both the currents is proposed, based on a motor model taking parasitic stray capacitors inside an induction motor into account. The common-mode current oscillation can be

TABLE I
TESTED INVERTER AND INDUCTION MOTOR RATINGS.

input voltage	3 ϕ 200	V
rated current	21.0	A
maximum current	52.0	A
modulation scheme	sinusoidal PWM	
carrier frequency	2.4	kHz
rated output	3.7	kW
rated torque	23.5	Nm
maximum torque	70.6	Nm
motor speed	1500/2000	r/min

perfectly damped by the common-mode transformer which has been proposed by the authors[2] while the normal-mode current oscillation can be damped by the normal-mode filters being proposed in this paper. The EMI radiated by a 3.7kW induction motor drive system is actually measured, complying with the VDE 0871 Class A [3m].

Experimental results verify that the combination of the common-mode transformer and the normal-mode filters is a practically viable and effective way to reduce the EMI resulting from both the common-mode and normal-mode currents.

II. SYSTEM CONFIGURATION

Fig.1 shows the configuration of an experimental system. An induction motor of 3.7kW is driven by a voltage-source PWM inverter through three feeding wires. The motor frame is connected to a virtual grounding point through a grounding wire. A 10m long 5.5mm² wide copper wire is used as each feeding wire and the grounding wire. Table I shows the tested inverter and induction motor ratings.

A common-mode transformer and three normal-mode filters are connected to the inverter output terminals. The common-mode transformer is the same as a conventional common-mode choke except for adding a secondary winding shorted by a resistor of R_t , intended for damping of the common-mode current oscillation[2]. Each normal-mode filter consists of parallel connection of an inductor of L_f and a resistor of R_f , intended for damping of the normal-mode current oscillation. The common-mode current dissipates a small amount of active power in the resistor of R_t , while the normal-mode current dissipates a negligible

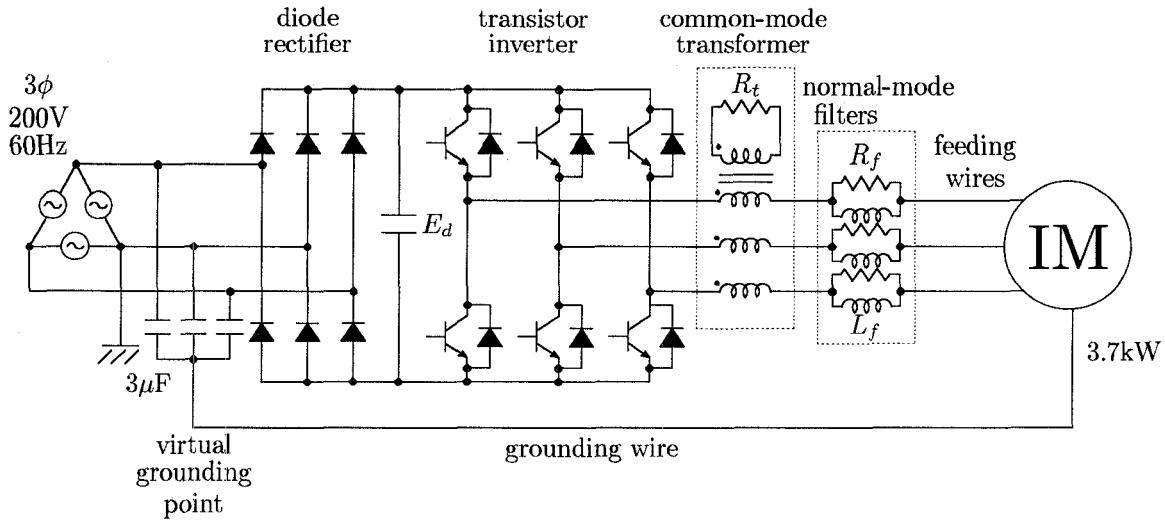


Fig. 1. System configuration.

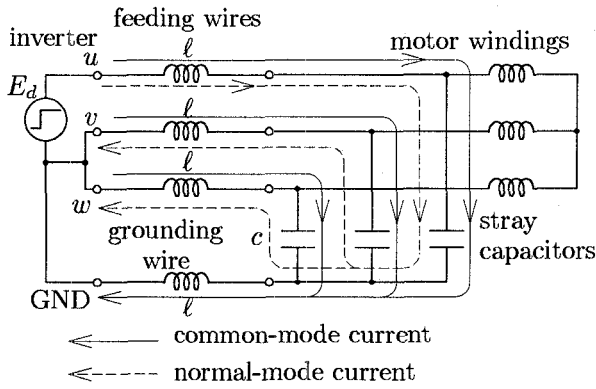


Fig. 2. Motor model including stray capacitors.

amount of active power in the resistor of R_f .

A virtual grounding point is introduced to avoid the influence of an internal impedance between the earth terminal on the switch board and the actual grounding point[2]. Three capacitors with a capacitance value being much larger than the stray capacitance in the motor, are connected to the three-phase ac terminals of the diode rectifier: The grounding wire is connected to the neutral point of the three capacitors, which is considered a virtual grounding point. In the experimental system, the capacitors of $3\mu F$ are used for providing the virtual grounding point.

III. COMMON-MODE AND NORMAL-MODE CURRENTS

Fig.2 shows a motor model taking the stray capacitors inside the motor into account[2]. The stray capacitors are represented by three capacitors in the motor model, c . The stray capacitor between a stator winding and the motor frame has a capacitance value being larger than that between two stator windings, because the stator windings are embedded into slots of the stator core. Accordingly, any

stray capacitor between two stator windings is negligible. Here, ℓ means a line inductance of each feeding wire between the inverter and motor terminals.

Moreover, Fig.2 corresponds such a case that a switching from the lower to the upper potential of the dc link voltage, when the other two phases remain connected to the lower potential. Note that the GND terminal is connected to the lower potential, based on the following assumptions:

- The high-frequency common-mode impedance of the diode rectifier is negligible.
- The grounding wire and the feeding wires have a line inductor with the same inductance value.

After the switching, the dc link voltage of E_d is applied only to the u -phase terminal, thus increasing the common-mode voltage by $E_d/3$. Once a switching occurs in one phase of the inverter, a common-mode current and a normal-mode current can flow, which are depicted by the solid line and the dotted line, respectively, as shown in Fig.2. The common-mode current is also referred to as the zero-sequence current or the ground current escaping through the stray capacitors to the grounding wire. The normal-mode current flows from one phase, in which a switching occurs, to the other two phases.

The inductance and capacitance concerning the common-mode current shown as the solid line in Fig.2 are $L_c = \frac{4}{3}\ell$ and $C_c = 3c$, respectively. On the other hand, the circuit loop for the normal-mode current shown as the dotted line has an inductance of $L_n = \frac{3}{2}\ell$ and a capacitance of $C_n = \frac{2}{3}c$. Table II summarizes the circuit parameters which have relation to the common-mode and normal-mode currents. The ratios of voltage, characteristic impedance and resonant frequency can be calculated as $1/3$, $4/9$ and $1/2$, respectively. This implies that the normal-mode current has the amplitude four-third times as large as the common-mode current, and has the oscillatory frequency twice as high as the common-mode current.

TABLE II
COMMON-MODE AND NORMAL-MODE.

item	L	C	E	Z	ω
common-mode	$\frac{4}{3}\ell$	$3c$	$\frac{1}{3}E_d$	$\frac{2}{3}\sqrt{\ell/c}$	$\frac{1}{2}\frac{1}{\sqrt{\ell c}}$
normal-mode	$\frac{3}{2}\ell$	$\frac{2}{3}c$	E_d	$\frac{3}{2}\sqrt{\ell/c}$	$\frac{1}{\sqrt{\ell c}}$
ratio $\left(\frac{\text{common}}{\text{normal}}\right)$	$\frac{8}{9}$	$\frac{9}{2}$	$\frac{1}{3}$	$\frac{4}{9}$	$\frac{1}{2}$

L : inductance Z : characteristic impedance
 C : capacitance ω : resonant frequency
 E : voltage

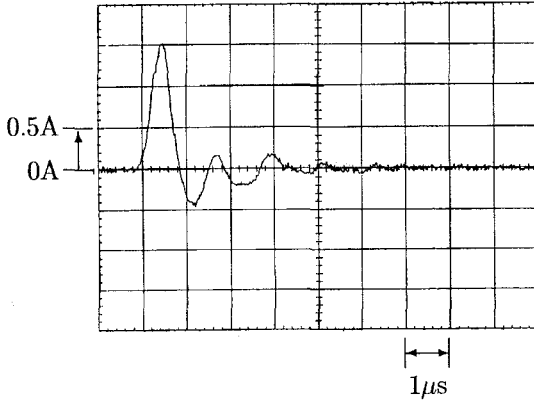


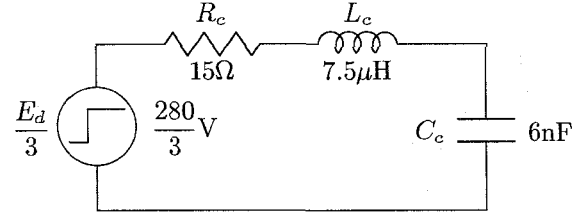
Fig. 3. Common-mode current waveform without common-mode transformer.

IV. COMMON-MODE TRANSFORMER

Fig.3 shows an actually measured waveform of the common-mode current or the ground current escaping through the grounding wire, when a switching occurs in a phase of the PWM inverter. Neither the common-mode transformer nor the normal-mode filters are connected in Fig.3. A nonnegligible amount of common-mode current flows through the stray capacitors, which has a peak value of 1.5A with an oscillation frequency of 750kHz under the rated motor current of 21.0A.

Fig.4 shows an equivalent circuit for the common-mode current, which forms an LCR series resonant circuit. A switching in one phase causes a step change of the common-mode voltage by $1/3$ of the dc link voltage. The circuit parameters are estimated from the experimental waveform shown in Fig.3, considering the rise-time of 340ns in the inverter output voltage.

In order to reduce the common-mode current, the common-mode transformer proposed by the authors in reference [2] is connected to the inverter output terminals. The common-mode transformer is the same as a conventional common-mode choke except for adding a tightly coupled secondary winding, the terminals of which are shorted by a resistor. Although the common-mode current flowing in the three-phase feeding wires produces a flux in the fer-



resonant frequency: $f_c = 1/2\pi\sqrt{L_c C_c} = 750\text{kHz}$

characteristic impedance: $Z_c = \sqrt{L_c/C_c} = 35.4\Omega$

damping factor: $\zeta_c = R_c/2Z_c = 0.212$

Fig. 4. Equivalent circuit for common-mode current.

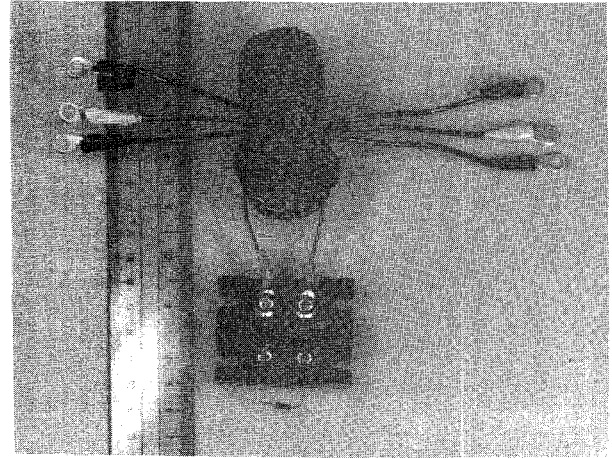


Fig. 5. Common-mode transformer.

rite core, no flux is created by the inverter output current other than it. Therefore, the common-mode transformer acts as damping resistor only for the common-mode current, i.e., the ground current.

According to the already proposed design method [2], a prototype common-mode transformer is designed and built for the experimental system. Fig.5 shows the photograph of the common-mode transformer. A damping resistor of 0.5W is connected to the secondary winding terminals because a negligible amount of power would be dissipated in the resistor. Fig.6 shows the equivalent circuit for the common-mode current in case of connecting the Common-Mode Transformer (CMT). Because its leakage inductance is negligible, the common-mode transformer is represented by a magnetizing inductor connected in parallel with the damping resistor. The inductance and resistance values are decided as 6.4mH and 510Ω, respectively.

Fig.7 shows an actually measured waveform of the common-mode current in case of connecting the common-mode transformer. Comparing Fig.7 with Fig.3 concludes that the peak value of the common-mode current is reduced to $1/8$, but also that the perfect damping of the common-mode current oscillation is achieved by the common-mode

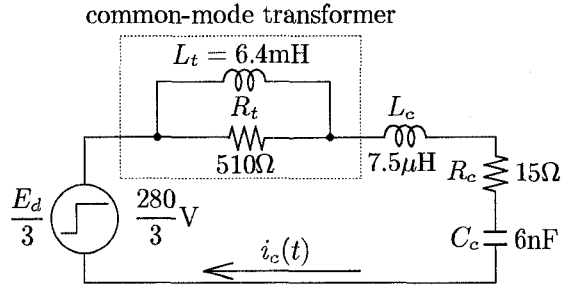


Fig. 6. Equivalent circuit for common-mode current in case of connecting CMT.

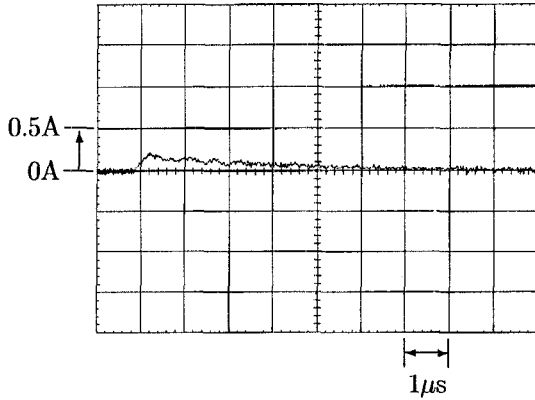


Fig. 7. Common-mode current waveform in case of connecting CMT.

transformer.

V. NORMAL-MODE FILTERS

Fig.8 shows a measured waveform of the inverter output current in a phase the moment a switching occurs in the corresponding phase. A nonnegligible amount of the normal-mode current is superimposed on the motor current along with $1/3$ of the common-mode current shown in Fig.3. The oscillatory component or the normal-mode current in the inverter output current has the peak value of 2A and the oscillatory frequency of 1.5MHz. Hence, the normal-mode current may cause not only the EMI but also ringing and overvoltage at the motor terminals. Comparing the normal-mode current oscillation with the common-mode current oscillation leads to the fact that the peak value and oscillation frequency ratios are $4/3$ and 2 , respectively. The experimental results coincide with the analytical results shown in Table II.

Fig.9 shows an equivalent circuit for the normal-mode current, which forms an LCR series resonant circuit. A switching in one phase causes a step change of the normal-mode voltage by the dc link voltage. Like the circuit parameters in the common-mode equivalent circuit, those in Fig.9 are estimated from the experimental waveform shown in Fig.8, considering the rise-time of 340ns in the inverter

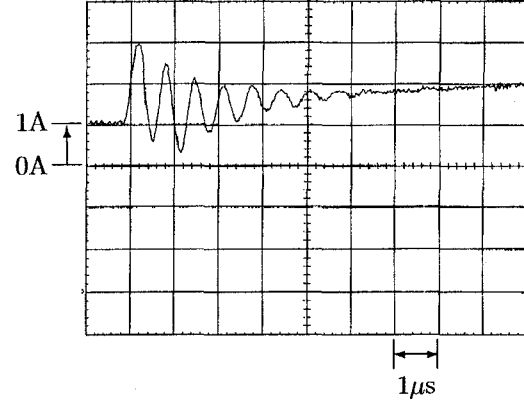
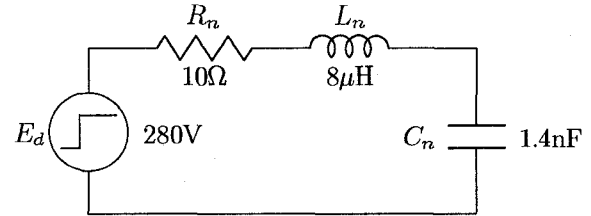


Fig. 8. Inverter output current waveform superimposing normal-mode current on motor current, without normal-mode filters.



$$\text{resonant frequency: } f_n = 1/2\pi\sqrt{L_n C_n} = 1.50\text{MHz}$$

$$\text{characteristic impedance: } Z_n = \sqrt{L_n/C_n} = 75.6\Omega$$

$$\text{damping factor: } \zeta_n = R_n/2Z_n = 0.066$$

Fig. 9. Equivalent circuit for normal-mode current.

output voltage.

These circuit values are compared with those in the Fig.4. The inductance ratio $L_c/L_n = 0.94$ and the capacitance ratio $C_c/C_n = 4.3$ also approximate $8/9$ and $9/2$ shown in Table II, respectively. This verifies that the motor model of Fig.2 is capable of dealing with both the common-mode and normal-mode currents.

In order to damp the normal-mode current oscillation, a resistor has to be inserted in series with the normal-mode current loop. However, the series insertion of the resistor results in consumption of a large amount of power, because not only the high-frequency oscillatory current i.e. the normal-mode current but also the non-oscillatory motor current flows through the resistor. Three normal-mode filters, each of which consists of a resistor and an inductor, are connected between the inverter and motor terminals, so that only the high-frequency oscillatory current flows through the resistor while the inverter output current other than it flows in the inductor. This justifies the series insertion of the resistor for damping of the normal-mode current oscillation.

Fig.10 shows the normal-mode equivalent circuit, including the normal-mode filters. The form of the normal-mode equivalent circuit is quite the same as that of the common-mode equivalent circuit shown in Fig.6. This indicates that

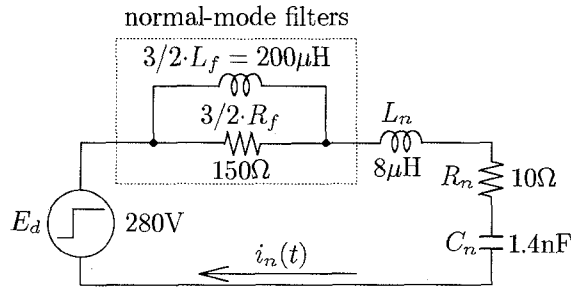


Fig. 10. Equivalent circuit for normal-mode current in case of connecting normal-mode filters.

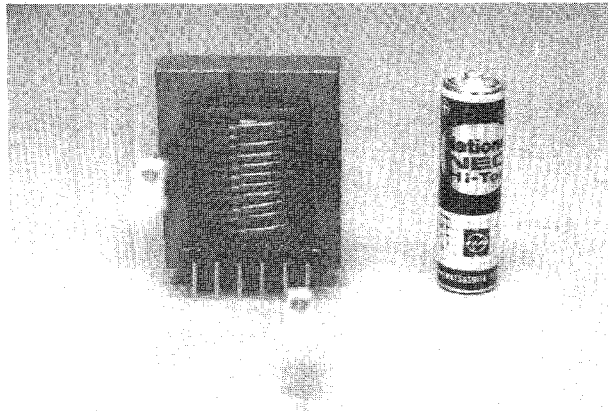


Fig. 11. Normal-mode filter inductor used for experiment.

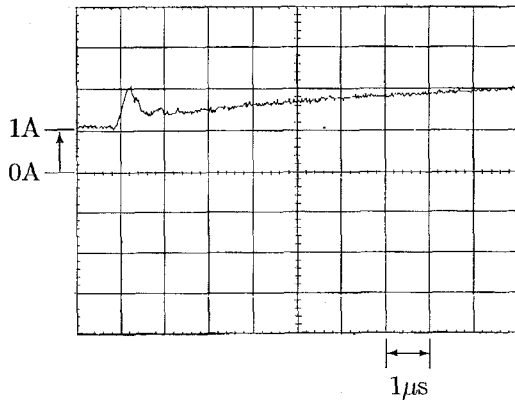


Fig. 12. Inverter output current waveform in case of connecting normal-mode filters.

the method of designing the common-mode transformer[2] is applicable to the normal-mode filters.

To damp the normal-mode current oscillation, the following condition should be satisfied.

$$2Z_{n0} < \frac{3}{2}R_f < \frac{1}{2}Z_{n\infty} \quad (1)$$

Here,

$$Z_{n0} = \sqrt{\frac{L_n}{C_n}}, \quad Z_{n\infty} = \sqrt{\frac{3}{2} \frac{L_f}{C_n}}. \quad (2)$$

Therefore, the normal-mode filter inductance is decided as $133\mu\text{H}$, because L_f should be larger than $16\frac{3}{2}L_n = 85\mu\text{H}$. Fig.11 shows an actual inductor used in the normal-mode filter. A resistor of 100Ω is connected in parallel to the inductor. The cutoff frequency of the normal-mode filter is calculated by

$$\frac{R_f}{2\pi L_f} = 120\text{kHz}. \quad (3)$$

The normal-mode filter acts as a resistor of 100Ω in a much higher frequency range than the cutoff frequency, while it acts as an inductor of $133\mu\text{H}$ in a much lower frequency range.

Fig.12 shows the experimental waveform of the inverter output current in case of connecting the normal-mode filters. The peak value of the normal-mode current is reduced to 1A, and the normal-mode current oscillation is perfectly damped by the normal-mode filters.

VI. MEASUREMENT OF EMI

Fig.13 shows a schematic diagram of the EMI measurement performed in a semi-anechoic chamber. All drive system appliances are placed on the basement under the chamber except for the induction motor, in order to measure only the EMI caused by the high-frequency oscillatory currents flowing in the grounding wire and the feeding wires between the inverter and motor terminals. All the wires are fixed along a wooden frame of $1\text{m} \times 1\text{m}$. The measurement is performed, based on four different wiring ways;

- A. to make the three feeding wires and the grounding wire up into a bundle,
- B. for the ground wire separated from the feeding wires to form a nonnegligible circuit loop,
- C. for the intentionally wrong wired u -phase feeder to form a nonnegligible circuit loop,
- D. to use a shielded three-core cable, the shielding conductor of which is used as the grounding wire.

Fig.14 shows the tested induction motor and the wooden frame for experiment and measurement. The motor is put on a wooden desk. In wiring A, the feeding wires and the grounding wire are fixed together along the upper and right sides of the wooden frame. In wiring B or C, either the grounding wire or the u -phase feeding wire is fixed along the left and lower sides of the frame, thus forming a circuit loop. In wiring D, the shielded conductor used as the grounding wire is connected between the motor frame and the virtual grounding point.

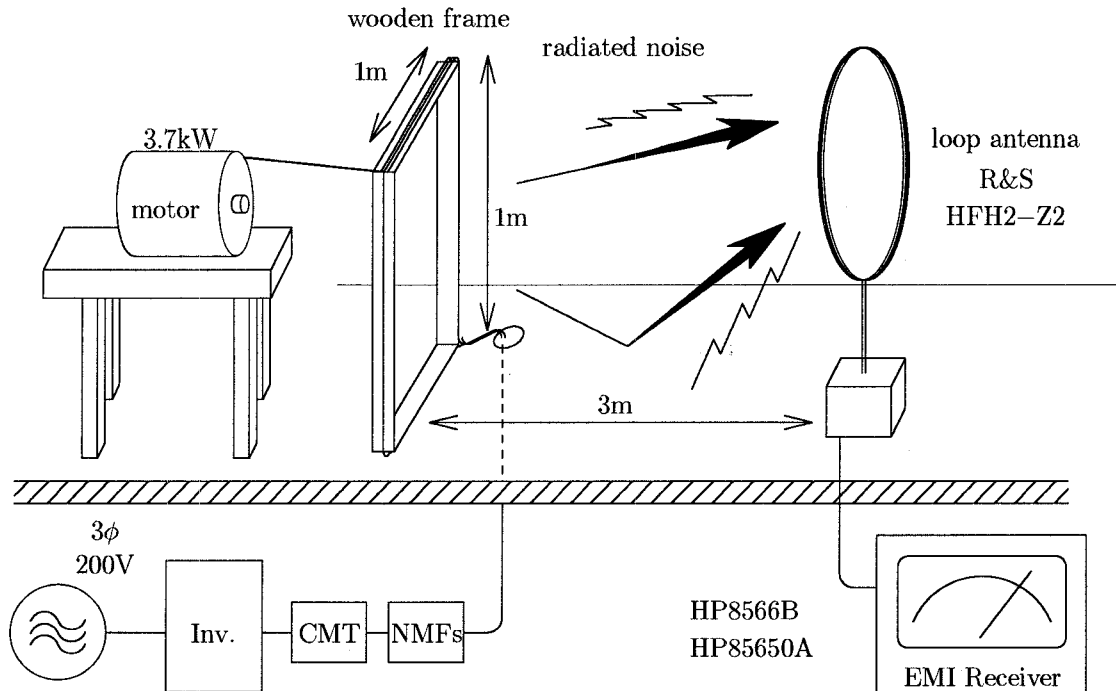


Fig. 13. EMI measurement.

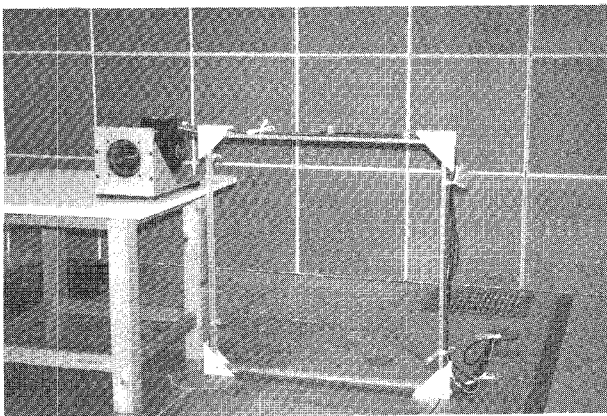


Fig. 14. Measurement situation.

Fig.15 shows the measured result of the radiated EMI in wiring **A**, without common-mode transformer and normal-mode filters. The radiated EMI does not exceed the limit value although the common-mode and normal-mode currents flow together. The radiation is negligible because the magnetic field produced by the currents is canceled each other.

Fig.16 shows that in wiring **B**, without common-mode transformer and normal-mode filters. The wiring **B** corresponds to the general wiring condition that the three-phase feeding wires are made up a bundle while the motor frame

is connected to a ground terminal through the grounding wire "separated" from the bundle. Hence, each phase common-mode current flowing in the circuit loop formed by the feeding wires and the grounding wire can radiate the EMI. However, the normal-mode current can hardly radiate the EMI although it flows in the feeding wires. Fig.16 concludes that the EMI in a range from 150kHz to 1MHz exceeds the limit value by 15dB.

Fig.17 shows that in wiring **C**, without common-mode transformer and normal-mode filters. The common-mode current and the normal-mode current flow in the *u*-phase wire, where the *u*-phase common-mode current is equal to 1/3 of the ground current. Therefore, the EMI produced by the common-mode current in the range from 150kHz to 1MHz is smaller than that of Fig.16 by about 10dB. The EMI produced by the normal-mode current has a peak at 1.5MHz, and the peak value exceeds the limit value by 15dB. The peak frequency coincides with the resonant frequency of the normal-mode equivalent circuit shown in Fig.9. The measured results shown in the above three figures indicate that both the common-mode and normal-mode currents can radiate the EMI. Minimizing the loop area formed by the feeding and/or grounding wires, however, is effective in reducing the radiated EMI.

Fig.18 shows the measured result of the EMI in wiring **D**, without common-mode transformer and normal-mode filters. The result indicates that the use of the shielded three-core cable is more effective in suppressing the radiated EMI. Note that the shielded cable tends to have higher capacitance between each inner wire and the shielding con-

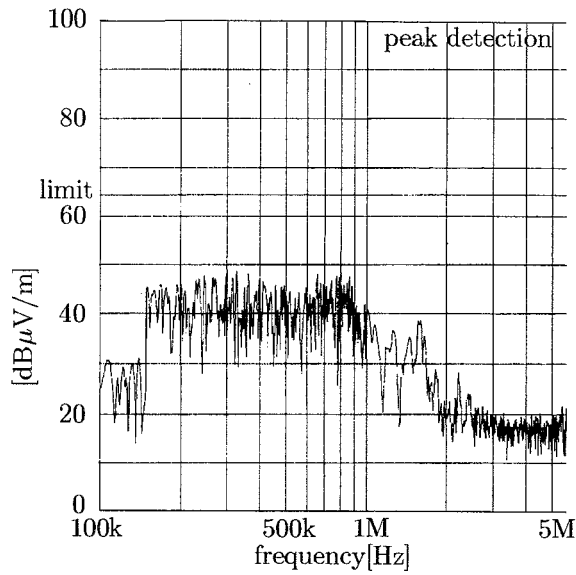


Fig. 15. Radiated EMI (wiring A).

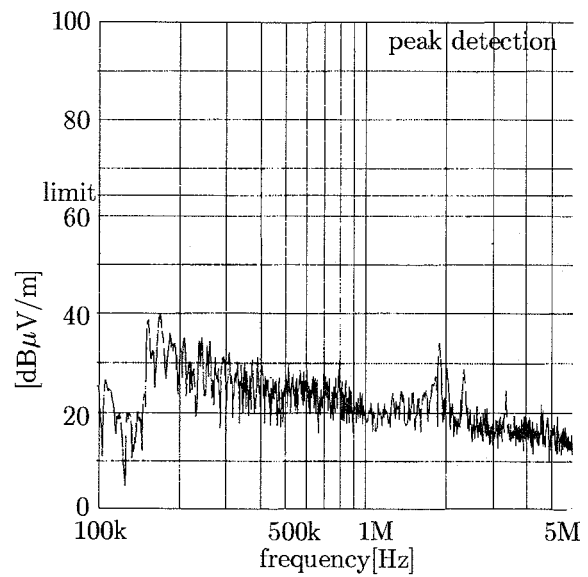


Fig. 18. Radiated EMI (wiring D).

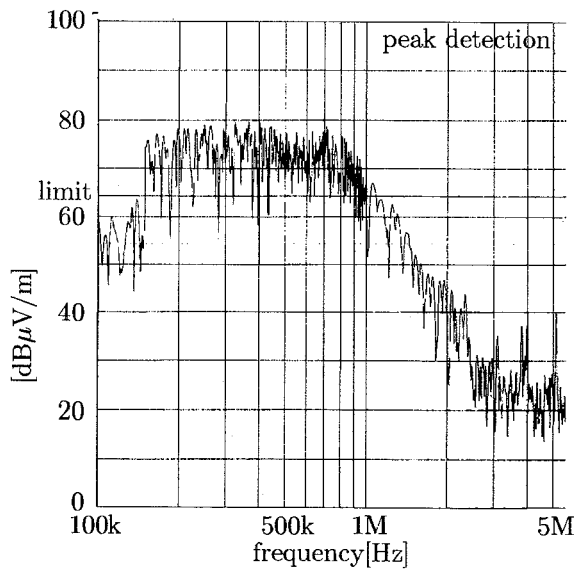


Fig. 16. Radiated EMI (wiring B).

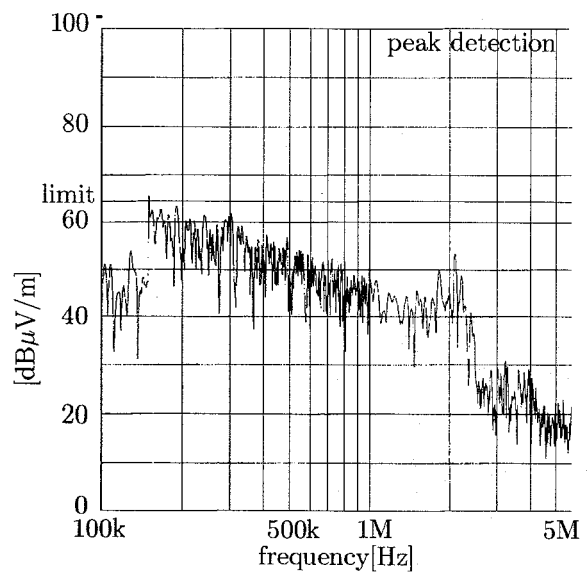


Fig. 19. Radiated EMI with CMT and NMFs (wiring B).

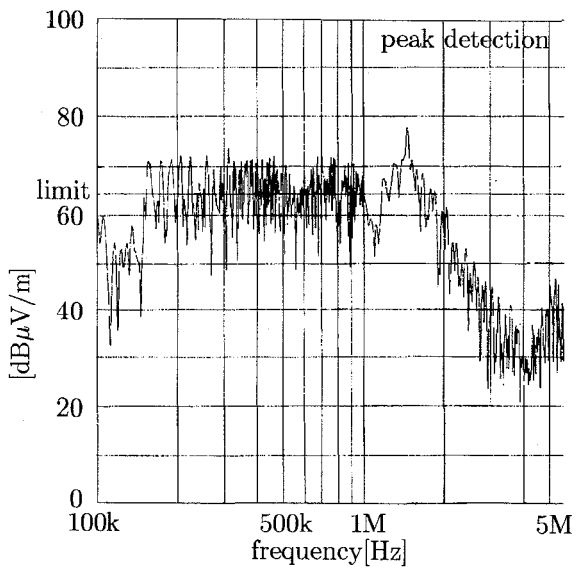


Fig. 17. Radiated EMI (wiring C).

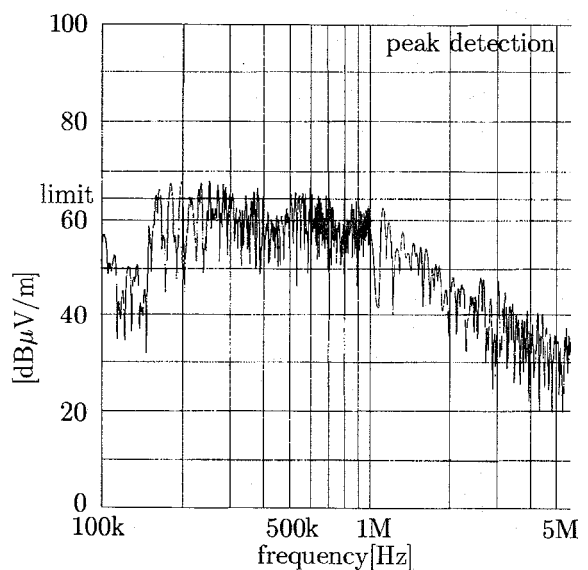


Fig. 20. Radiated EMI with CMT and NMFs (wiring C).

ductor.

Fig. 19 shows that of the EMI in wiring B, with both the common-mode transformer and the normal-mode filters. Compared with Fig. 16, the EMI in the range from 150kHz to 1MHz decreases by 20dB, because the common-mode transformer can damp the common-mode current oscillation as shown in Fig. 7. In this case, the EMI is suppressed within the limit value.

Fig. 20 shows that in wiring C, with both the common-mode transformer and the normal-mode filters. The peak at 1.5MHz in Fig. 17 perfectly disappears in Fig. 20 because of excellent damping effect of the normal-mode filters shown in Fig. 12.

VII. CONCLUSION

This paper has discussed the theoretical and experimental relationships between the EMI radiated throughout and the high-frequency oscillatory currents flowing through the stray capacitors inside an induction motor. The experimental results have led to the following conclusions:

- The motor model described in Fig. 2 is capable of dealing with both the common-mode and normal-mode currents.
- The equivalent circuit for either the common-mode or normal-mode current is represented by an LCR series resonant circuit.
- Connecting both the common-mode transformer and the normal-mode filters between the inverter and motor terminals is a practically viable and effective way, not only of damping the common-mode and normal-mode current oscillation, but also of reducing the EMI radiated by the current oscillation.
- The use of a shielded three-core cable is more effective in reducing the radiated EMI than minimization of the loop area formed by the feeding wires and the grounding wire, although the oscillatory currents flow out from the inverter terminals.

The common-mode transformer and the normal-mode filters would be expected to solve other problems such as the conducted EMI, insulation life and bearing current.

REFERENCES

- [1] Y. Murai, T. Kubota, and Y. Kawase: "Leakage Current Reduction for a High-Frequency Carrier Inverter Feeding an Induction Motor", *IEEE Trans. Industry Applications*, vol. 28, no. 4, pp. 858-863, Jul./Aug., 1992.
- [2] S. Ogasawara and H. Akagi: "Modeling and Damping of High-Frequency Leakage Currents in PWM Inverter-Fed AC Motor Drive Systems," *IEEE/IAS Annual Meeting*, pp. 29-36, 1995.
- [3] M. A. Jabbar and M. A. Rahman: "Radio Frequency Interference of Electric Motor and Associated Controls," *IEEE Trans. Industry Applications*, vol. 27, no. 1, pp. 27-31, Jan./Feb., 1991.
- [4] G. Venkataramanan and D. M. Divan: "Pulse Width Modulation with Resonant dc Link Converters," *IEEE Trans. Industry Applications*, vol. 29, no. 1, pp. 113-120, Jan./Feb., 1993.
- [5] E. Zhong, S. Chen, and T. A. Lipo: "Improvement in EMI performance of inverter-fed motor drives," in *APEC 94 Conf. Rec.*, pp. 608-614, vol. 2, 1994.
- [6] S. Chen, T. A. Lipo, D. Fitzgerald: "Modeling of Motor Bearing Currents in PWM Inverter Drives," *IEEE/IAS Annual Meeting*, pp. 388-393, 1995.
- [7] J. M. Erdman, R. J. Kerkman, D. W. Schlegel and G. L. Skibinski: "Effect of PWM Inverters on AC Motor Bearing Currents and Shaft Voltages," *IEEE Trans. Industry Applications*, vol. 32, no. 2, pp. 250-259, Mar./Apr., 1996.
- [8] B. Heller, A. Veverka: "Surge Phenomena in Electrical Machine", ILIFFE BOOKS LTD., 1968.
- [9] R. E. Pretorius and A. J. Eriksson: "A basic guide to rc surge suppression on motors and transformers", *Transaction on SA Institute of Electrical Engineers*, pp. 201-209, Aug. 1980.
- [10] B. K. Bose: "Power Electronics and Motion Control - Technology Status and Recent Trends," *IEEE Trans. Industry Applications*, vol. 29, no. 5, pp. 902-909, Sep./Oct., 1993.
- [11] A. von Jouanne, D. Rendusara, P. Enjeti, W. Gray: "Filtering Technique to Minimize the Effect of Long Motor Leads on PWM Inverter Fed AC Motor Drive Systems," *IEEE/IAS Annual Meeting*, pp. 37-44, 1995.